Automated Measurement of Backlash and Stiffness in Electro-Mechanical Flight Control Actuation

SCHALLERT Christian
German Aerospace Center (DLR e.V.)
Institute of System Dynamics and Control
82234 Wessling, Germany
Phone: +49 (0) 8153 28 2408
Email: christian.schallert@dlr.de

ROTTACH Michael
Liebherr-Aerospace Lindenberg GmbH
Pfaenderstrasse 50-52
88161 Lindenberg, Germany
Phone: +49 (0) 8381 46 6542
Email: michael.rottach@liebherr.com

KOWALSKI Robert
German Aerospace Center (DLR e.V.)
Institute of Flight Systems
38108 Braunschweig, Germany
Phone: +49 (0) 531 295 3652
Email: robert.kowalski@dlr.de

DORKEL André
Liebherr-Aerospace Lindenberg GmbH
Pfaenderstrasse 50-52
88161 Lindenberg, Germany
Phone: +49 (0) 8381 46 5633
Email: andre.dorkel@liebherr.com

ABSTRACT

Electro-mechanical actuation of primary flight control surfaces is expected to increase the efficiency of future commercial aircraft. More specifically, the effort and cost of manufacture and maintenance will be reduced due to the omission of hydraulic supply and actuation systems. However, backlash is inherent to electro-mechanical actuation, whereas it does not occur in conventional hydraulic servo-actuation. Due to wear, backlash increases over the lifetime. With regard to electro-mechanical actuation of primary flight control surfaces, excessive backlash can cause detrimental effects such as limit cycle oscillations or, as a worst case, lead to jamming. Therefore, efficient and simple-to-deploy methods for monitoring backlash are sought after.
This paper describes time domain methods for automated measurement of backlash and stiffness that use available sensor signals of an electro-mechanical aileron actuation system. So far, feasibility of the methods has been verified by experiments on appropriate test benches.

KEYWORDS

automated measurement, backlash, electro-mechanical actuation, primary flight control, stiffness

I INTRODUCTION

The backlash measurement methods described in this paper are developed for, but not limited to, an electro-mechanical aileron actuation that consists of two identical, parallel actuators normally operated in an active-active manner. The methods are time domain and exploit some of the system's sensor signals available. Given signal accuracies suffice for the methods, hence no additional system requirements are involved.
Other related research is dedicated to frequency domain methods for backlash measurement (Tjahjowidodo et al., 2004), to optimisation-based system identification (Dalla Vedova et al., 2015) or to linear model approaches, e.g. Kalman filter, that identify the amount of backlash as a single non-linearity in a system (Hovland et al., 2002), (Lagerberg and Egardt, 2003). (van der Linden and Dorkel, 2017) use a Kalman filter based approach to detect bearing or gear wheel defects in an EMA.
Here, two backlash measurement methods are introduced. One of them, called **BLFserv**, is intended for continuous monitoring of backlash when the actuation system operates in service. The other method, called **BLFmaint,** is devised as an automated maintenance check that can be performed on the ground only.
The methods have been conceived and implemented by the DLR Institute of System Dynamics and Control (DLR-SR), in collaboration with the DLR Institute of Flight Systems (DLR-FT) and Liebherr-Aerospace Lindenberg (LLI) in the frame of the German *LuFo V-1 EMA* research project. DLR-FT have set up and operated a so called active-active test rig

(see Figure 2) that replicated the flight surface actuation including aerodynamic loads. The main purpose of this test rig was to examine force fight controllers developed for the synchronous operation of two parallel EMAs. In addition, testing of the backlash measurement methods was performed. LLI, as an aircraft systems manufacturer, have provided EMA hardware to the test rig as well as guidance and background information to this common effort. What is more, LLI have provided measurement data recorded at another rig that operated a single EMA for endurance testing. Therefore, a multitude of datasets from both test rigs has been considered in the development and tuning of the measurement algorithms. Also, they were run on the rigs' real-time systems in order to check their capability.

This paper is organised as follows: The dual EMA actuation system and according test rig are described in 1.1. Methods **BLFmaint** and **BLFserv** are described in 2.1 and 2.2, respectively; 2.3 includes a measurement accuracy analysis.

1.1 Brief System Description

Figure 1 shows a schematic of the dual EMA flight surface actuation. Each EMA comprises a motor (M), a reduction gear, a ballscrew and nut (ram) on the output side that is connected to the surface. The housing side is attached to the wing's rear spar. Both ends are fitted with spherical bearings to prevent any constraining forces. The surface is deflected around its hinge axis by accordant motion of both EMAs. Altogether, a closed mechanical chain is formed that shows backlash and stiffness.

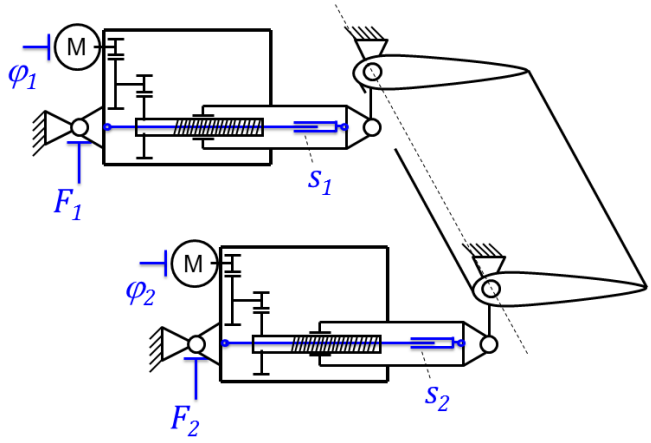

Figure 1. System schematic

To measure these characteristics, the sensors marked blue in the schematic are used. φ_1 and φ_2 denote the motor axis angles. Each is picked up by a resolver, i.e. a rotary electrical transformer. The analogue angle signals are converted to 12 bit wide binary signals. In addition, consecutive phase shifts of the angle signals are accounted for in the computing of φ_1 and φ_2. s_1 and s_2 are the actuator strokes that are measured between the housing and the ram by Linear Variable Differential Transducers (LVDT). LVDTs are electrical transformers used for metering translational displacement. F_1 and F_2 are the EMA forces. On the test rigs, these are measured by load cells mounted adjacent to the EMA housing side. For the aircraft system, instrumented bolts, so called load pins, are designed.

Figure 2 shows an image of the active-active test rig that reproduces the relevant mechanical characteristics and kinematics of the actuation system depicted in Figure 1. The rig comprises two EMAs connected to a common, rigid shaft that has an inertia representative of the flight surface. Aerodynamic loads are imposed on this shaft by two hydraulic cylinders. The overall stiffness of the real flight surface mechanism (including the surface's torsional and the attachment stiffnesses) is replicated by two adjustable spring elements, each placed between the rig structure and the EMA housing side. All sensors signals necessary are available at a sample rate of 500 Hz.

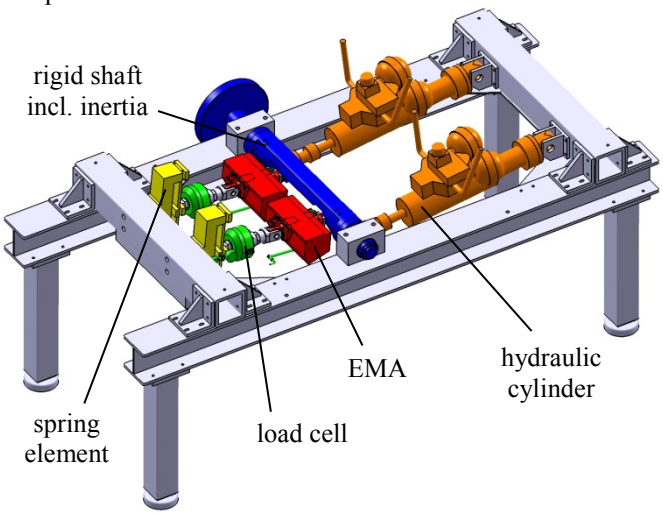

Figure 2. Active-Active test rig with two EMAs

II BACKLASH FILTER METHODS

In 2.2, method **BLFserv** is described that uses the motor angle and ram position signals in order to determine the backlash between an EMA's motor shaft and its output side. This is referred to as internal backlash. In addition, the so called external backlash can be determined by comparison of the ram position signals of the two parallel EMAs.

Any sensor-based method can measure backlash only if it is traversed. This can occur, for instance, due to inertia effects if the flight surface is moved back and forth in a normal manner. No experiment or specific motion of the surface is required for method **BLFserv**. Therefore, it is suitable as a continuous in service backlash monitor.

Method **BLFmaint** described in 2.1 is devised as an automated maintenance check. It requires small opposite excursions of the two parallel EMAs. The load signals (that are used for force-fight control) are evaluated in addition to the position signals. Thus, internal and external stiffness can be measured as well.

Attention has been paid in the development of both methods to the given sensor accuracies, including calibration errors, and the hence achievable measurement accuracy. It shall be better by one order of magnitude than the internal and external backlash that are normally in the order of 0.1mm.

2.1 Measurement on Maintenance – BLFmaint

BLFmaint exploits the motor angle φ_1, φ_2, ram position s_1, s_2 and force signals F_1, F_2 in order to measure backlash and stiffness. The method draws on a force F versus difference D relationship, where

$$D_{int,1} = s_1 - \frac{\varphi_1}{i_{total}}, \qquad D_{int,2} = s_2 - \frac{\varphi_2}{i_{total}} \qquad \text{and}$$
$$D_{ext} = s_2 - s_1 \qquad (1)$$

are the internal (EMA) and external (surface mechanism) position differences. i_{total} is the EMAs' total mechanical gear ratio in $\left[\frac{rad}{mm}\right]$.

Figure 3 shows data of an experiment on the active-active test rig in which the EMAs were stressed up to ±15% of their limit load. This has been achieved by an according demand input to the force-fight control loop that generated small opposite excursions of both EMAs. (This experiment does not reflect normal operation of the actuation system, where force-fight is minimised.) The upper diagram shows the variation of force F_1 in time, the lower diagram the according $D_{int,1}$ signal. The vertical axes are scaled by the actuator limit load F_{limit} and specified backlash B_{spec}, respectively.

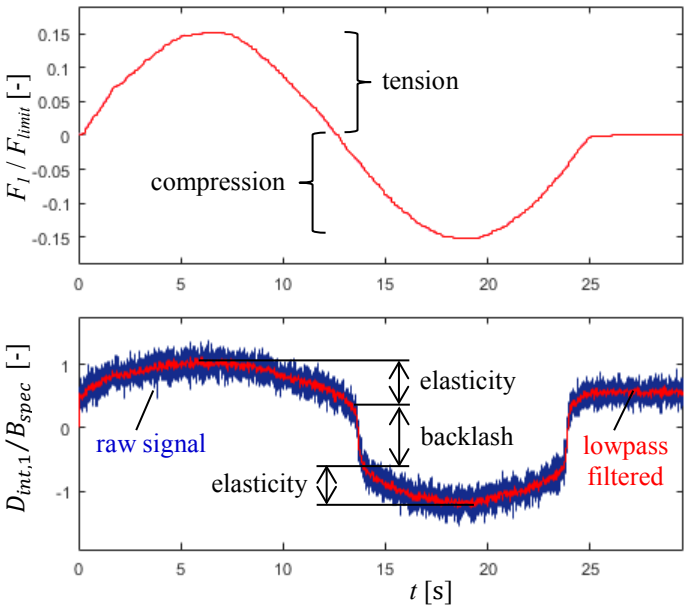

Figure 3. EMA1 force F_1 and internal difference $D_{int,1}$ versus time t during an active-active test rig experiment

Backlash appears as a jump of the D signal, here $D_{int,1}$. After it has been traversed and all components of an EMA's load path are in contact, elastic behaviour is evident. It is important that, although the transition from elasticity to backlash or reverse is not sharp (visco-elasticity), both methods, **BLFmaint** and **BLFserv**, can distinguish between them.

To this end, **BLFmaint** divides the recorded F versus D data into three parts – tension, backlash and compression – as shown by the vertical dashed lines in Figure 4. In doing so, the derivative $\frac{dF}{dD}$ is numerically computed, filtered and its median determined. This is shown in the lower part of Figure 4. The median, i.e. statistical mean value, is used instead of the arithmetic mean value, because it is less distorted by extremely large or small values. Such extremes occur in the derivative $\frac{dF}{dD}$ due to measurement noise. The median is negative for the data shown, since force F_1 globally decreases with increasing difference $D_{int,1}$. Next, the range is determined that extends farthest in x-axis direction where the derivative $\frac{dF}{dD}$ is larger than its median. This range is confined by the two intersections of $\frac{dF}{dD}$ with the median. They are named D_{lc} and D_{rc}, as shown.

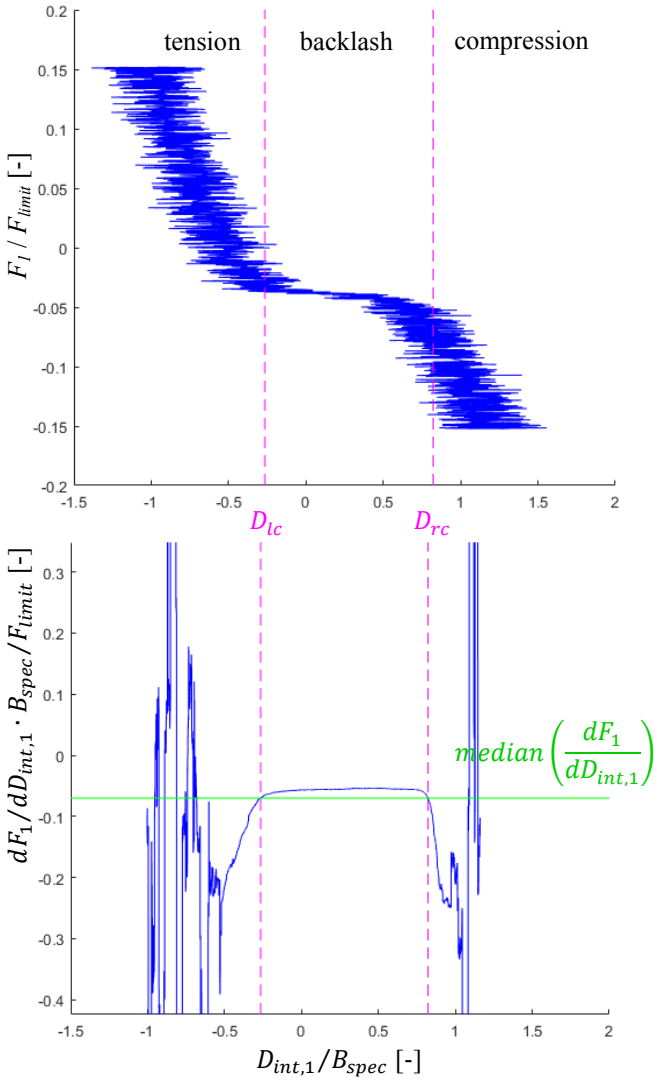

Figure 4. Force F_1 and derivative $dF_1/dD_{int,1}$ versus internal difference $D_{int,1}$ for the data shown in Figure 3

That followed, a linear regression of the recorded F versus D data is performed for each of the three parts delimited by D_{lc} and D_{rc}. This approach assumes, for simplicity, linear tensile and compressive stiffness of an EMA. The corresponding regression lines are depicted in Figure 5. Backlash B is determined as the horizontal distance of the intersections of c_{left} with c_{center} and c_{center} with c_{right}, as indicated.

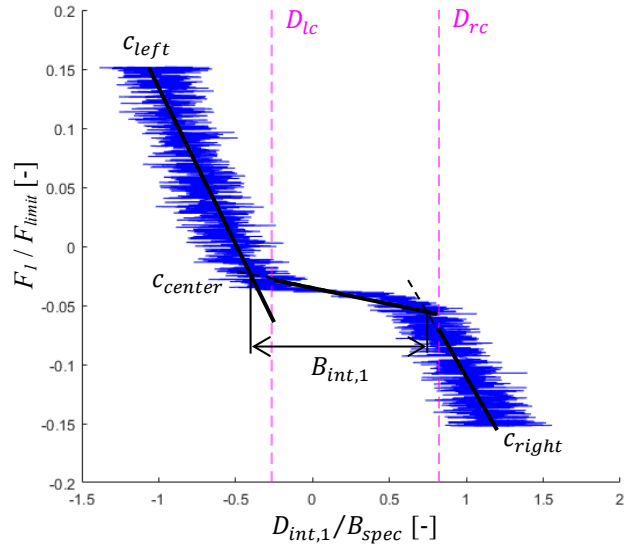

Figure 5. Internal backlash $B_{int,1}$ and stiffness c_{left}, c_{right} determined using the data shown in Figure 3

In addition, method **BLFmaint** is capable of determining the external backlash and stiffness, which refers to the flight surface mechanism, except the EMAs. To this end, the force fight $F_2 - F_1$ versus external position difference D_{ext} (1) is evaluated. This is depicted in Figure 6 for the same test rig experiment as analysed before. In comparison to Figure 5, it shows that the overall external stiffness c_{left}, c_{right} is lower by multiples than the internal stiffness, which is a plausible and expected result. The external backlash B_{ext} determined is in the same order of magnitude as the internal backlash.

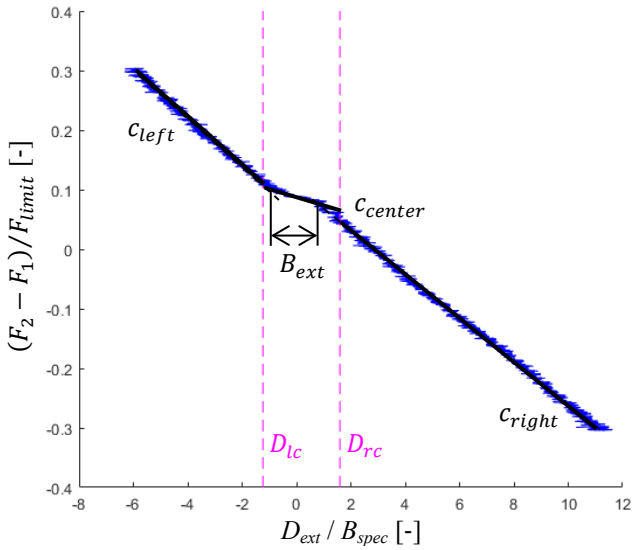

Figure 6. External backlash and stiffness determined for the same test rig experiment as shown in Figure 3

2.2 Continuous Measurement – BLFserv

Figure 7 shows data of an experiment on the active-active test rig in which the actuation went through the full stroke s_{full} at full rate. The force-fight compensation was active, so this experiment represents a normal operating case.

Backlash appears as short-time jumps of the computed position difference D (1). Therefore, method **BLFserv** has been developed to trace such jumps and measure their height. This avoids that elastic deformation is included in the backlash values. The respective D signal is lowpass filtered $filter_{LP}(\dots)$ for noise attenuation and differentiated with respect to time $filter_{DT1}(\dots)$ in order to detect jumps:

$$D_{filtered} = filter_{LP}(D) \qquad (2)$$

$$\dot{D} = filter_{DT1}(D_{filtered}), \quad \ddot{D} = filter_{DT1}(\dot{D}) \qquad (3)$$

where $D = D_{int,1}$, $D = D_{int,2}$ or, respectively, $D = D_{ext}$.

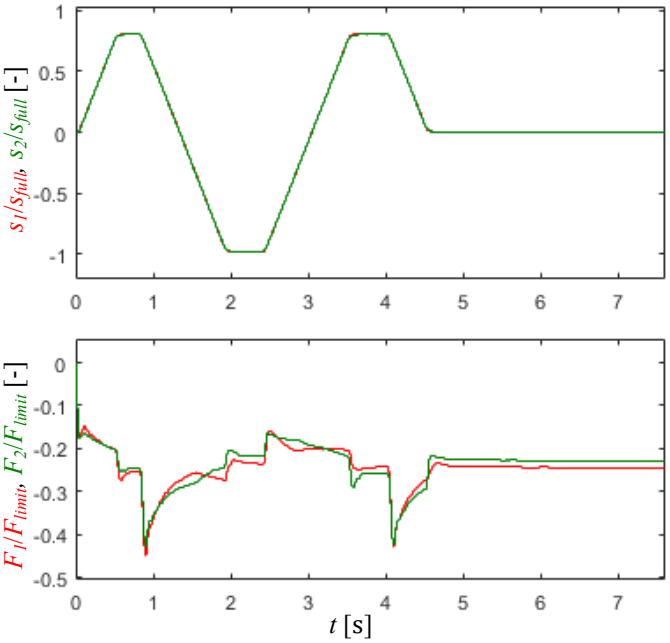

Figure 7. EMA strokes s and forces F during another active-active test rig experiment (normal operation)

Other than **BLFmaint**, **BLFserv** draws on the ram position s and motor angle φ signals only; force signals are not evaluated. Thus, **BLFserv** lends itself also to actuation that does not include force sensors, e.g. spoiler surfaces.

Figure 8 shows the evaluation for EMA1 of the experiment indicated in Figure 7. The left and right columns include the same signals, in which the right column is zoomed in direction of the time axis. The filtered first and second derivatives $\dot{D}_{int,1}$, $\ddot{D}_{int,1}$ (3) of $D_{int,1}$ are shown in the lower diagrams. When backlash is traversed, both derivatives exceed the threshold zone delimited by $\{-thresh, thresh\}$, as marked in the lower right corner of Figure 8. Then, the change of $D_{int,1}$ is recorded as $\Delta D_{int,1}$ from the time instant when both derivatives exceed the threshold zone until the time instant when the first or second derivative (or both) returns into it. Eventually, the largest amplitude of $\Delta D_{int,1}$ is issued as backlash $B_{int,1}$, as the mid diagrams show.

It is necessary to compute and evaluate the second $\ddot{D}$ in addition to the first derivative $\dot{D}$, because variation of the first derivative can occur without the backlash actually traversed. Elastic deformation or large and rapid actuator movement, in combination with inaccurate calibration of the ram LVDTs, can produce such effect.

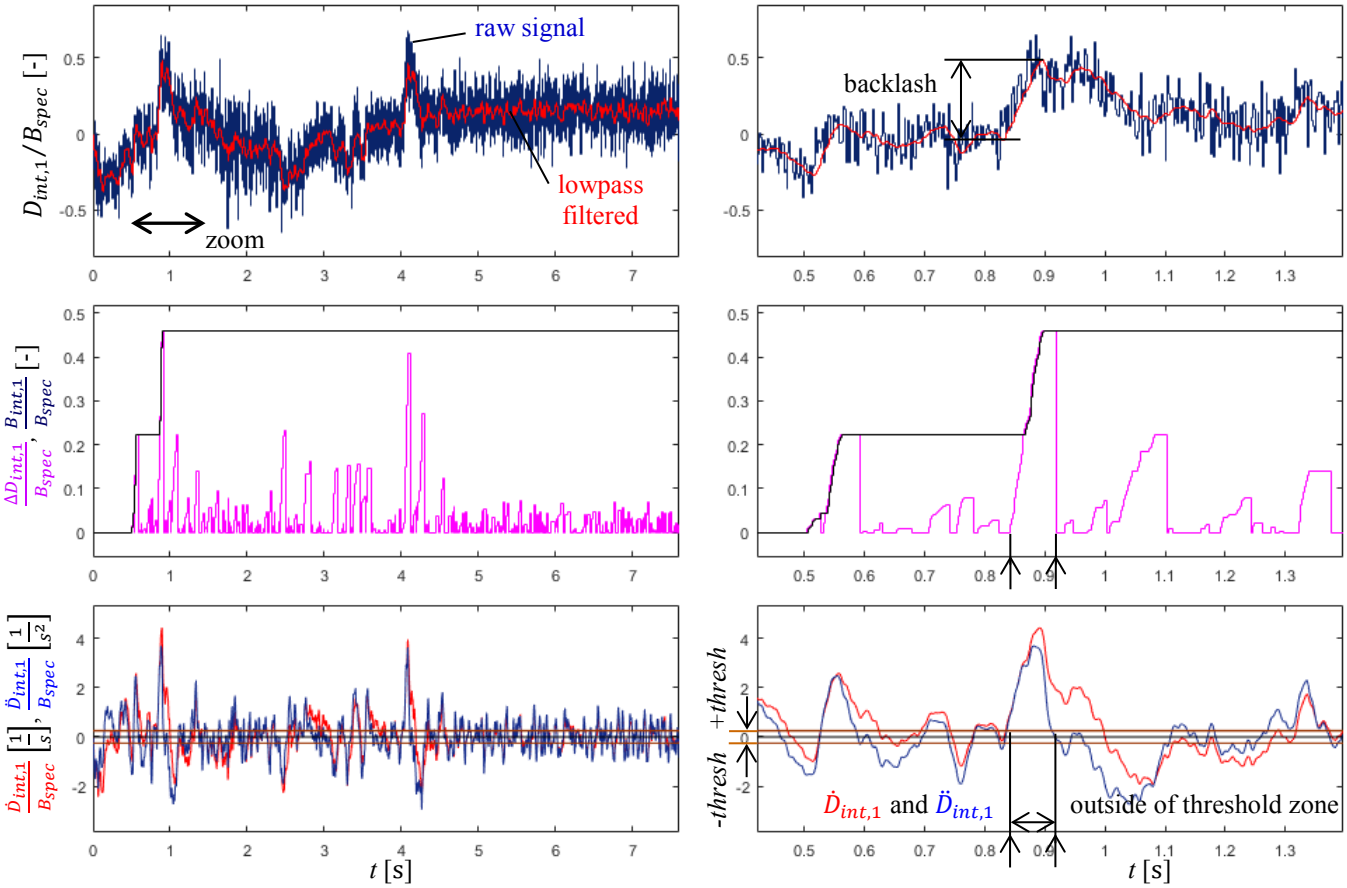

Figure 8. Internal backlash of EMA1 measured by method **BLFserv** for the experiment shown in Fig. 7

2.3 Accuracy of Backlash Measurement

The backlash measurement accuracy can be affected by LVDT calibration error, noise and temperature influence.

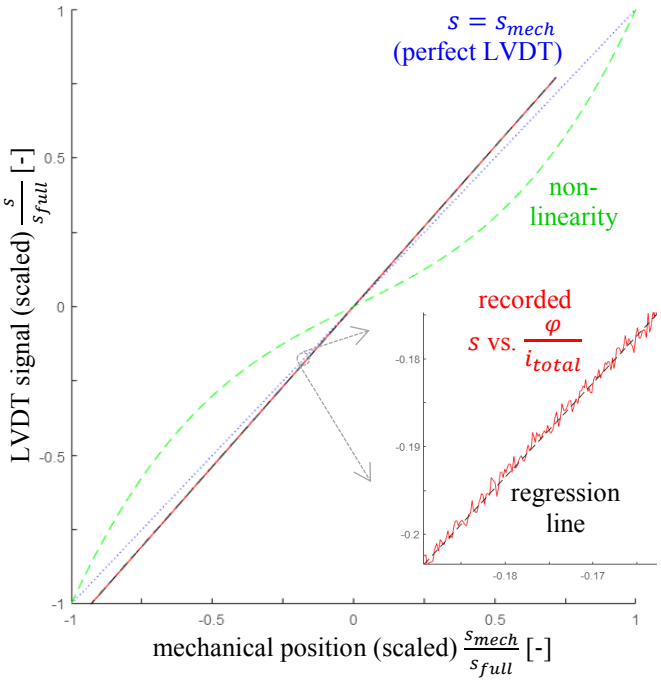

Figure 9. Compensation of LVDT calibration errors

Calibration error means that the LVDT signal is systematically biased from the actual stroke. Pitch and offset errors, or non-linearity are conceivable, as shown in Figure 9. Calibration errors can be compensated. To this end, a dedicated adjustment procedure is carried out in which the full stroke is slowly passed through while a constant opposing force is applied. Then, a regression is performed on the recorded LVDT signal s, i.e. the ram position, versus motor angle $\frac{\varphi}{i_{total}}$ data. (The motor angle is divided by the EMA's total gear ratio to refer it to the ram.) For one EMA on the active-active test rig, this has revealed a necessary correction of the pitch by $s = \frac{1}{1.075} \cdot s_{mech}$, as Figure 9 shows. Given the full mechanical stroke s_{full} of the actuation of ±20mm, a non-compensated pitch error of 7.5% would lead to a backlash measurement error of ±20mm·0.075 = ±1.5mm. Without this compensation, such unreasonably high backlash values were actually measured when the test rig actuation went through full stroke. Expected backlash values are normally in the order of 0.1 mm.

Figure 9 also shows that the regression of the recorded data is almost perfect (overall root mean square error <0.02). Thus, the LVDT calibration error is fully compensated, and the backlash measurement is not affected.

Measurement noise with a 0.025 mm peak to peak amplitude is seen in the LVDT signals as well. Lowpass filtering with a

crossover frequency of 40 rad/s is used for attenuation, as can be seen in Figure 3 and Figure 8.
Temperature changes cause a systematic, not random LVDT signal error. This has to be considered due to the actuation's wide operating temperature range. A maximum signal error of 1% can be assumed for LVDTs of the used kind. Since the repetitive error of an LVDT is virtually zero at a constant temperature, the 1% error is related to temperature changes. Method **BLFserv** meters jumps of the computed difference D that can originate from the LVDT signal. Such jumps will reasonably not exceed a tenth of the full mechanical stroke, i.e. ±2mm. Thus, backlash measurement error will not exceed $\pm 2\text{mm} \cdot 0.01 = \pm 0.02\text{mm}$, which is one order of magnitude less than the expected values. Method **BLFmaint** is intended as a maintenance check on the ground. The adjustment procedure for compensation of LVDT calibration errors and the **BLFmaint** procedure are performed one after another, all automated. Therefore, no change of ambient temperature and hence no effect on the backlash measurement will occur.

CONCLUSION

Two methods for sensor-based automatic backlash measurement in electro-mechanical actuation have been introduced. The methods are developed for, but not limited to, an aileron actuation that consists of two parallel, synchronously operated EMAs. Method **BLFserv** is intended as a continuous in service monitor. Since it uses motor angle and ram position signals only, it is suited for other applications as well, e.g. single EMA spoiler surface. Method **BLFmaint** is devised as a maintenance check that requires a specific motion of the actuation. It can be used only for dual actuation systems that include load sensors. In return, stiffness is measured as well.
Analysis has shown that a backlash measurement accuracy of better than 0.1mm can be achieved using the sensors available, which is sufficient for the intended use case. In addition, a series of test rig experiments has confirmed that the repeatability is in the order of 0.01mm for internal or external backlash measurement. Interestingly, measurement values of **BLFserv** are lower by about a quarter than those of **BLFmaint**. Yet, this is a known, systematic deviation that results from the methods' different evaluation principles.
Both methods have proven to work on test rigs, i.e. under laboratory conditions. It remains to be verified that they give precise results also under environmental conditions that are representative of aircraft operation.

REFERENCES

Dalla Vedova M. D. L., Lauria D., Maggiore P. and Pace L. (2015), *Linear Electromechanical Actuators affected by Mechanical Backlash: A Fault Identification Method based on Simulated Annealing Algorithm*, WSEAS Transactions on Systems, Vol. 14 (2015) pp 268-277, E-ISSN: 2224-2678

Hovland G., Hanssen S., Moberg S., Brogardh T., Gunnarsson S. and Isaksson M. (2002), *Nonlinear Identification of Backlash in Robot Transmissions*, Proceedings of the 33rd ISR (International Symposium on Robotics), Stockholm, Sweden, October 7-11, 2002

Lagerberg A. and Egardt B. S. (2003), *Estimation of Backlash with Application to Automotive Powertrains*, Proceedings of the 42nd IEEE Conference on Decision and Control, Maui, Hawaii, USA, December 2003

van der Linden F. L. J. and Dorkel A. (2017), *Real-Time Model- and Harmonics based Actuator Health-Monitoring*, Proceedings of the 6th International Workshop on Aircraft System Technologies (AST 2017), pp 43-50, Hamburg, Germany, February 21-22, 2017

Tjahjowidodo T., Al-Bender F. and Van Brussel H. (2004), *Identification of Backlash in Mechanical Systems*, Proceedings of ISMA 2004 (International Conference on Noise and Vibration Engineering, pp 2195-2209, Leuven, Belgium, September 20-22, 2004

NOTATIONS

Symbols

B	backlash
c	stiffness
D	computed difference
F	EMA force
i	gear ratio
s	EMA stroke
φ	EMA motor angle

Subscripts

1	Actuator 1
2	Actuator 2
int	internal
ext	external
lc	left corner
mech	mechanical
rc	right corner
spec	specification

AKNOWLEDGEMENT

This research has received funding from the German government department of economy and technology in the frame of the *LuFo V-1 EMA PFC Subsystem* joint research project (LUFOV1-549-022, BMWi/LuFo 20Y1304B) that was conducted from 2014 to 2017.